

Article

# Aroma Profile of Grapevine Chips after Roasting: A Comparative Study of Sorbara and Spergola Cultivars for More Sustainable Oenological Production

Veronica D'Eusanio <sup>1,2,\*</sup> , Lorenzo Morelli <sup>1</sup>, Andrea Marchetti <sup>1,2,3</sup>  and Lorenzo Tassi <sup>1,2,3,\*</sup> 

<sup>1</sup> Department of Chemical and Geological Sciences, University of Modena and Reggio Emilia, 41125 Modena, Italy; lollo2200@gmail.com (L.M.); andrea.marchetti@unimore.it (A.M.)

<sup>2</sup> National Interuniversity Consortium of Materials Science and Technology (INSTM), 50121 Firenze, Italy

<sup>3</sup> Interdepartmental Research Center BIOGEST-SITEIA, University of Modena and Reggio Emilia, 42124 Reggio Emilia, Italy

\* Correspondence: veronica.deusanio@unimore.it (V.D.); lorenzo.tassi@unimore.it (L.T.)

**Abstract:** This study aimed to compare the aroma profiles of Sorbara and Spergola grapevine prunings roasted at different temperatures (120, 140, 160, 180, 200, and 240 °C). One potential application of grapevine prunings is their use as infusion chips to enhance and improve the aging processes of alcoholic beverages and vinegars. Aromatic compounds impart unique flavors and contribute to the complexity of the final products. Thermogravimetry–mass spectrometry coupled with evolved gas analysis (TGA-MS-EGA) was conducted to identify the thermal steps at which substantial changes occurred in the wood matrix. Solid-phase microextraction–gas chromatography–mass spectrometry (SPME-GC-MS) was used for the analysis of volatile compounds. Several key volatile compounds were identified, showing variations in their concentrations as a function of cultivar and roasting temperature. Furan derivatives, such as furfural, and phenolic compounds, such as guaiacol and vanillin, were the two main chemical classes of volatile compounds that predominantly defined the aroma of grapevine chips roasted above 180 °C. At lower roasting temperatures, some aldehydes, such as hexanal and terpenes, defined the aroma profiles of the samples. By repurposing waste materials, this application offers a pathway for environmentally conscious viticulture and sustainable practices within the food industry.

**Keywords:** sustainability; roasted grape pruning; *Vitis vinifera*; aroma profile; HS-SPME-GC-MS; wine aging; waste management



**Citation:** D'Eusanio, V.; Morelli, L.; Marchetti, A.; Tassi, L. Aroma Profile of Grapevine Chips after Roasting: A Comparative Study of Sorbara and Spergola Cultivars for More Sustainable Oenological Production. *Separations* **2023**, *10*, 532. <https://doi.org/10.3390/separations101100532>

Academic Editor: Rosaria Costa

Received: 27 July 2023

Revised: 25 September 2023

Accepted: 27 September 2023

Published: 6 October 2023



**Copyright:** © 2023 by the authors. Licensee MDPI, Basel, Switzerland. This article is an open access article distributed under the terms and conditions of the Creative Commons Attribution (CC BY) license (<https://creativecommons.org/licenses/by/4.0/>).

## 1. Introduction

The current climate crisis highlights the pressing need for sustainable practices across various sectors of the economy, including viticulture. As environmental concerns intensify, there is an increasing recognition of the significance of utilizing waste materials and embracing innovative approaches to mitigate environmental impact. In this context, grapevine pruning, which represents a substantial byproduct of the vineyard industry, offers a wealth of untapped potential for sustainable applications.

The viticulture sector generates a significant amount of agricultural waste [1,2], with grapevine pruning as the main by-product [3]. Traditionally, these materials have been regarded as mere residues that are often left on the vineyard floor or burned. When left in the field, grapevine prunings can actually contribute to improve soil quality. They increase organic matter content, act as a nutrient source, and improve soil texture and structure. On the other hand, burning agricultural residues, including grapevine prunings, poses potential hazards due to the release of dangerous and persistent compounds, such as polycyclic aromatic hydrocarbons (PAHs) and greenhouses. PAHs, such as benzopyrene,

catechol, hydroquinone, phenanthrene, and naphthalene, have been associated with an increased risk of cancer in humans and animals. They are mutagenic, carcinogenic, and teratogenic [4]. Additionally, the burning of agricultural residues contributes to the release of anthropogenic  $N_xO_y$  and other gases, thereby contributing to global warming [5]. Given these environmental health concerns, there is growing recognition of the need to explore alternative uses of grapevine prunings [6]. These residues have gained significant attention because of their rich content of bioactive molecules, notably stilbenes [7], which function as phytoalexins in vine plants [8]. Phytoalexins are essential molecules that play critical roles in protecting plants against pathogenic microorganisms. Among these bioactive compounds, *trans*-resveratrol and *trans*- $\epsilon$ -viniferin have been extensively studied for their wide-ranging health benefits in humans, including anticancer, cardioprotective, and antioxidant effects [9,10]. Additionally, they exhibit antifungal properties and serve as natural preservatives in wine production [11]. In addition to stilbenes, vine prunings also contain other secondary metabolites, such as flavonoids (catechin and epicatechin) [12], as well as compounds released by lignin, particularly phenolic acids. These additional compounds further contribute to the nutritional and therapeutic value of vine prunings, thereby emphasizing their overall significance.

One particularly promising avenue is the utilization of grapevine prunings for aging wines, vinegars, and other alcoholic beverages [6]. By converting these prunings into infusion chips, they can serve as an alternative method to accelerate the aging process that typically occurs within traditional wooden barrels. This innovative approach not only offers an environmentally sustainable solution but also presents opportunities for enhancing the sensory attributes and complexity of the final products. The concept of using grapevine prunings as infusion chips for aging alcoholic beverages aligns with the principles of circular economy and waste valorization. By repurposing this agricultural waste, the viticulture industry can effectively reduce its environmental footprint, decrease its reliance on conventional aging materials, and contribute to the overall sustainability of the sector. Furthermore, the use of grapevine prunings as a renewable resource aligns with broader societal goals of transitioning towards a more resource-efficient and environmentally conscious future and with the goals of Agenda 2030 for Sustainable Development [13]. In addition to their potential as sustainable aging agents for alcoholic beverages and vinegars, grapevine prunings offer benefits in terms of terroir expression and flavor development. Prunings from specific grape cultivars contain unique aromatic compounds and chemical precursors that can contribute to the sensory characteristics of the final product. Therefore, investigating the aroma profiles and sensory attributes of different cultivars at varying roasting temperatures is crucial for harnessing the full potential of grapevine pruning as a sustainable and flavor-enhancing resource.

This study aimed to explore the aroma profiles of two distinct Lambrusco cultivars typical of the territory of Modena, the red-berry Sorbara and the white-berry Spergola, roasted at different temperatures. By characterizing the released aromatic compounds, we sought to identify the key flavor contributors and evaluate their suitability in enhancing the sensory experience of wine and other alcoholic beverages. Through this research, we aim to bridge the gaps among sustainable viticulture practices, flavor innovation, and environmental responsibility. Since the volatile organic compounds (VOCs) released by a material are closely related to its chemical composition [14–16], it is crucial to evaluate the proximate composition of our samples before assessing their volatile composition following roasting. This step is important for obtaining a comprehensive interpretation of the results of HS-SPME-GC-MS analysis. Understanding the chemical composition provides insights into potential precursors and pathways for the formation of VOCs during thermal treatment. Furthermore, each component within the sample may exhibit distinct behavior when subjected to thermal stress. Therefore, to gain a deeper understanding of the thermal characteristics of the samples, thermogravimetric analysis coupled with mass spectrometry (TG-MS-EGA) was employed. This comprehensive analysis technique provides valuable information about the thermal behavior of our samples, enabling us

to identify the specific temperature ranges at which different compounds decompose or undergo chemical transformations.

## 2. Materials and Methods

### 2.1. Sample Preparation

The woody stems of *Vitis vinifera* cultivars Lambrusco Sorbara (SO) and Spergola (SP) were collected from a farm in the Modena (Italy) territorial district, where these grapevines were cultivated under consistent soil, climate, and water regime conditions. To ensure the accuracy of the analytical procedures, we specifically chose the internal sections of the grapevine canes, excluding any parts that could potentially be contaminated by pesticides and fungicides. To eliminate potential contamination, the outer layer was carefully peeled off and manually removed.

Sampling was carried out in September 2022, and the pruned canes were air-dried at room temperature for one week. All samples were manually dehulled, minced, and reduced to chips 4–5 mm in size. They were then placed in closed glass containers and subjected to thermal treatment in a laboratory oven (Argo LAB, Carpi, MO, Italy) for 2 h at different temperatures (120, 140, 160, 180, 200, 220, and 240 °C) in an inert atmosphere (N<sub>2</sub>). The temperature and thermal contact times are factors, and their levels were derived from a preliminary design of experiments (DOE) model acquired beforehand and applied to these types of real matrices. The model's response correlates factors and levels to identify a range of values where the process approaches optimization. To create an inert atmosphere, a glass capillary was inserted into the vial, and nitrogen (N<sub>2</sub>) was flowed for 15 min to displace all atmospheric air, before quickly sealing the vial with its screw cap. To ensure consistency, a standardized set of samples was prepared as follows: approximately 1 g of material was transferred to 10 mL glass vials, which were sealed tightly with Teflon/silicone septa. The set of samples consisted of three replicates for each sample type (for each thermal treatment). The samples were promptly analyzed after preparation to characterize the VOC fraction.

### 2.2. Proximate Composition

The moisture, ash, elemental analysis, and crude protein content were determined following the methods recommended by the Association of Official Analytical Chemists [17]. The moisture content was determined by drying 600–700 mg of the samples at 105 °C to a constant weight. The ash content was determined using a laboratory furnace at 550 °C, and the temperature was gradually increased. Each measurement was performed in triplicate, and the results were averaged.

### 2.3. TGA-MS-EGA

A Seiko SSC 5200 thermal analyzer (Seiko Instruments Inc., Chiba, Japan) was used to conduct thermogravimetric analysis (TGA) under an inert atmosphere (He). A coupled quadrupole mass spectrometer (ESS, GeneSys Quadstar 422) was used to analyze the gases released during the thermal reactions (MS-EGA) (ESS Ltd., Cheshire, UK). Sampling was achieved through an inert and fused silicon capillary system, which was heated to prevent condensation. The intensity of the signal of selected target gases was collected in multiple ion detection mode (MID); a secondary electron multiplier operating at 900 V collected, in multiple ion detection mode (MID), the intensity of the signal of selected  $m/z$  target gases. The signal intensities of specific  $m/z$  ratios of 18 for H<sub>2</sub>O, 44 for CO<sub>2</sub>, 39 for the furfural fragment C<sub>3</sub>H<sub>3</sub><sup>+</sup>, and 60 for acetic acid were measured, respectively, where  $m/z$  is the ratio between the mass number and the charge of the ion. The heating conditions were 20 °C/min in the thermal range of 25–1000 °C using ultrapure He at a flow rate of 100 µL/min as the purging gas.

#### 2.4. Volatile Organic Compounds Sampling: HS-SPME

A solid-phase micro-extraction (SPME) holder (Supelco, Inc., Bellefonte, PA, USA) was used to conduct the SPME headspace (HS) analysis manually. Prior to analysis, all samples were subjected to 30 min of sonication in a thermostatic bath at  $40.0 \pm 0.1$  °C to favor the transfer of volatile compounds from the matrix to the headspace. After this step, volatiles were extracted by manually exposing a 2 cm long SPME fiber composed of DVB/CAR/PDMS (Supelco, Bellefonte, PA, USA) to the HS of the vial for 15 min at the same temperature of 50 °C. Finally, the fiber was withdrawn and inserted into the injector port of the GC-MS system to desorb the analytes at 250 °C.

Reproducibility of the experimental procedures was ensured by analyzing three replicates of the same matrix and collecting three different measurements for each vial. The three measurements within each vial were averaged to obtain a representative value. Subsequently, the average values from the three vials belonging to the same sample at each temperature were further averaged. Averaging the measurements within each vial reduced the impact of random fluctuations, whereas averaging across the vials for the same sample helped to minimize the influence of any sample-specific variations.

After chromatographic analysis of five real samples, blank tests were conducted. These tests involved the analysis of an external solution containing 1-decanol (conc. of 150 µg/g ethanolic solution) to assess any potential contamination or instrument performance issues.

#### 2.5. GC-MS Analysis

GC-MS analysis of the extracted volatile compounds was conducted using an Agilent 6890N Network gas chromatograph system coupled with a 5973N mass spectrometer (Agilent Technologies, Santa Clara, CA, USA). A DB-5MS UI column (60 m × 0.25 mm i.d., 1.00 µm film thickness; J&W Scientific, Folsom, CA, USA) was used, and He was employed as the carrier gas at a flow rate of 1.0 mL/min. SPME injection was performed in splitless mode. After 90 s, the purge vent was switched on, allowing a flow rate of 100 mL/min. After 10 min, the gas saver option was activated, setting a flow rate of 30 mL/min. The detector began to operate immediately after each injection. The column temperature was increased from 40 °C to 270 °C at a rate of 6 °C/min. The transfer line was heated to 270 °C.

The mass spectrometer operated in electron impact (EI) ionization mode at 70 eV, using the full scan acquisition mode with an *m/z* scanning range from 25 to 300.

The chromatograms and mass spectra were analyzed using Enhanced ChemStation software (Agilent Technologies, Santa Clara, CA, USA). The putative identification of volatile compounds was achieved by comparing the mass spectra with the data system library (NIST14/NIST05/WILEY275/NBS75K) and by using databases accessible via the web, such as the National Institute for Standards and Technology (NIST database <https://webbook.nist.gov> accessed on 12 March 2023) and the Mass Bank of North America (<https://mona.fiehnlab.ucdavis.edu> accessed on 12 March 2023).

Certain analytes were identified by comparing their mass spectra with those of their respective pure standards (when available) and analyzed by HS-SPME-GC-MS under the same operating conditions used for the samples. The multi-standard solution was prepared as follows: a volume of 10 µL of each analyte was extracted using a micro-syringe and introduced into a vial containing 10 mL of ethanol. The resulting homogenized solution was used for a duplicate test. Initially, 2 µL of sample was injected into the GC, yielding a fully resolved chromatogram of the analytes. The subsequent test aimed to determine potential interferences with matrix analytes. A volume of 1 µL of the solution was drawn using a GC syringe, introduced into a vial containing a sample of chips roasted at 180 °C for both cultivars. After equilibrating the vial's HS atmosphere, the SPME fiber was exposed, followed by GC analysis as described above. The results demonstrate the absence of any interference.

Volatile compounds, such as silane and siloxane derivatives, or volatile organic compounds related to the sorbent fiber were excluded and are not reported in the GC-MS output

tables. The amount of each volatile identified in the SPME-GC-MS analysis is expressed as the total ion current (TIC) peak area.

All data presented in the tables correspond to the values obtained from the analysis performed in triplicate. The reproducibility of the results is expressed as the standard deviation (SD) in the tables. The asterisk at the apex indicates an  $SD < 0.05$ .

### 2.6. Statistical Analysis

All measurements were performed in triplicate. The experimental data were compared using one-way analysis of variance (ANOVA) and Tukey's test. For each roasting temperature, a two-sample *t*-test was conducted to assess significant differences between the two cultivars. The level of significance was set at  $p < 0.05$  to determine whether there were statistical differences among the mean values. The statistical analyses were performed using the Matlab® 2023a environment (The Mathworks Inc., Natick, MA, USA).

### 2.7. Chemicals and Reagents

Propanal, 2-methyl-, hexanal; nonanal; 2-butanone; furfural; limonene; and 2-Furancarboxyaldehyde, 5-methyl-, guaiacol were obtained from Sigma-Aldrich products, distributed by Merck KGaA, Darmstadt, Germany. Acetone; methyl acetate; acetic acid; benzene; phenol; butyrolactone; 1-decanol; n-hexane; nonane; dodecane; tetradecane; and hexadecane were obtained from Carlo Erba Reagents, Milano (Italy). All the analytical standards had purity in the range of 95–99.8%.

## 3. Results

Roasting plays a pivotal role in enhancing the quality of vinegars and alcoholic beverages aged in wooden barrels, leading to a substantial increase in volatile compounds. This strong increase in volatiles is attributed to the thermal degradation of the wood, which triggers a cascade of chemical reactions. During roasting, wood undergoes thermolysis reactions, causing significant alterations in its chemical composition. The major biopolymers of wood, including lignin, cellulose, and hemicellulose, undergo breakdown and contribute to the transformation of its chemical structure [18–20]. This complex series of reactions imparts unique flavors, aromas, and sensory characteristics to the final product. Furthermore, roasted wood imparts desirable attributes, such as richness, complexity, and depth, elevating the overall quality and sensory experience of aged vinegars and alcoholic beverages. Figure 1 shows the samples from the Sorbara cultivar. The samples from the Spermogola cultivar did not exhibit appreciable differences in their appearance.



**Figure 1.** Grapevine chips from the Lambrusco Sorbara cultivar roasted at different temperatures (from left to right: 120, 140, 160, 180, 200, 220, and 240 °C).

The selection of temperatures aims to achieve a balance between maximizing desired and minimizing undesired effects. Temperatures that are too low might not produce enough aromatic compounds, whereas those that are too high could lead to the excessive formation of undesirable compounds or the loss of delicate volatile compounds. The selected temperatures constitute a representative range that allows for the exploration of a variety of potential aromatic impacts. Moreover, the choice of temperatures is supported by previous research through which information about the formation of aromatic compounds at different wood roasting temperatures has been obtained [21,22].

Regarding the potential application of grapevine wood as infused chips for aging alcoholic beverages and vinegars, some safety aspects should be considered. First, the removal of the outer bark reduces the risk of contamination by heavy metals, pesticides, and other contaminants. Previous studies have demonstrated the safety of ethanolic extracts of dehulled and roasted grapevine chips in terms of heavy metals [23]. Furthermore, with regard to pesticides and contaminants, grapevine pruning can be considered safe, as European regulations (Regulation (EC) No. 1107/2009 of the European Parliament and of the Council of 21 October 2009 [24,25]) mandate that pesticides used in grape cultivation must adhere to safety intervals between the last application and fruit harvest. Therefore, we can assume that the collection of grapevine prunings after grape harvest ensures phytosanitary safety.

### 3.1. Proximate Composition

The chemical composition and physical properties of vegetable matrices are known to be significantly influenced by various factors, such as geographical origin, degree of ripeness, and the specific cultivar [6]. Understanding the proximate chemical composition is crucial for determining the intrinsic properties of the samples under investigation. Table 1 presents the proximate chemical composition of the samples.

**Table 1.** Proximate chemical composition of Spergola and Lambrusco Sorbara grapevine canes.

	Spergola	Sorbara
Moisture % (at 105 °C)	23.1 ± 0.4	17.9 ± 0.1
Forced drying % (at 120 °C)	34.3 ± 0.2	38.4 ± 0.2
C % *	45.0 ± 0.1	46.6 ± 0.4
H % *	6.99 ± 0.07	6.94 ± 0.08
N % *	0.50 ± 0.04	0.47 ± 0.03
S % *	<0.1	<0.1
O% *#	44.5 ± 0.4	42.9 ± 0.5
Ash %	3.01 ± 0.04	3.07 ± 0.06
Cellulose §		~32–34
Hemicellulose §		~19–27
Lignin §		~26–28

\* On dry basis at 105 °C; # by difference; § from the literature data [26–29].

The water content in the white grape variety (Spergola) pruning was slightly higher, a finding supported by previous research [30]. Similar to other vegetable biomasses [31], grapevine canes are composed primarily of cellulose, which consists of glucan and is the most abundant biopolymer [32,33]. Hemicelluloses (mannans, xyloglucans, and xylans) followed cellulose in terms of abundance. The cellulose content in grapevine canes is approximately 32–34% on a dry basis [28], whereas the hemicellulose content ranges from 19 to 27%. The large variability observed might be related to differences in analytical procedures (extraction, analyses, and calculation) and/or variability among grape varieties [30]. Lignin, a high-molecular mass cross-linked polymer, constitutes approximately 26–28% on a dry basis and is composed of three major C6–C3 phenylpropanoid units (*trans*-p-coumaroyl, coniferyl, and sinapyl units), and characterized by a phenolic structure [12]. Grapevine canes also contain other compounds in smaller quantities, such as lipids and bioactive

molecules, including antioxidants, vitamins, tannins, and pigments. These compounds are interlaced within the polysaccharide and lignin matrix [34]. Vine canes also contain essential minerals, aroma compounds, and molecules with organoleptic properties [12,35]. The presence of ash was minimal, accounting for approximately 3% of the total composition. Among the various compounds found in vine canes, polyphenols have been extensively studied because of their antioxidant properties and beneficial effects on human health [6].

### 3.2. TGA-MS-EGA Analysis

Thermogravimetric analysis–mass spectrometry–evolved gas analysis (TGA-MS-EGA) is a powerful analytical technique that provides valuable information regarding the various degradative processes involving all constituents within an organic matrix, like grapevine wood. This enables the determination of the degradation characteristics of different components, the identification of reaction products, and the assessment of the thermal stability of specific constituents within the matrix. These processes often occur simultaneously, leading to a partial or total overlap in specific temperature ranges, which can be identified in the thermogram. In TGA-MS-EGA, the thermogram profile represents the sum of the various contributions from different degradative reactions occurring concurrently. Deconvoluting the signals and interpreting the thermogram can be challenging, particularly when different processes generate the same reaction products, such as H<sub>2</sub>O, CO, and CO<sub>2</sub>.

The analysis reported relates only to the Lambrusco Sorbara cultivar, as no significant differences were observed in comparison to the Spergola cultivar.

To effectively interpret the thermograms, the temperature range is typically divided into intervals of different sizes and characteristics. The values in Table 1 indicate that the total organic mass of the samples was 75–80%. Starches and simple sugars are usually present at trace levels in wood. Similarly, other compounds with high biological value, such as polyphenols and tannins, contribute minimally to the total organic mass. The protein content was also low, with a nitrogen content below 1%, as confirmed by several studies [6,23,36]. Therefore, our samples consisted mainly of primary indigestible fractions, including cellulose, hemicellulose, and lignin. The TGA results, along with its first derivative (DTG), were obtained in an inert atmosphere (He), as illustrated in Figure 2. The quantitative considerations related to these results are summarized in Table 2.

The degradation processes of the sample components lead to the formation of volatile organic compounds (VOCs), which constitute the volatile fraction and play a vital role in the development of the characteristic aroma of roasted wood. Thermogram analysis is crucial to acquire a comprehensive understanding of the complex phenomena that occur during the roasting process.

The thermogram domain is divided into five regions, each representing the behavior of the matrix in relation to some specific process. Region I covers the temperature range up to approximately 120 °C and can be attributed to the moisture removal phase, along with the simultaneous thermal elimination of particularly volatile organic compounds, which contribute to the characteristic aroma profile of the fresh matrix ( $-\Delta m\% = 3.3\%$ ). The initial consideration suggested by the thermogram in Figure 2 stems from the comparison with the moisture values in Table 1. The significant difference might originate from the quantity of samples processed using the different techniques and operational methodologies. TGA-MS-EGA was conducted with a small sample amount, 10–15 mg, to be compactly inserted into the Pt microcrucible in order to prevent or minimize thermal anisotropy phenomena. Nevertheless, the sample was expected to be representative of the rather heterogeneous starting matrix. Therefore, it cannot be ruled out that a combination of these factors (small mass and thermal anisotropy) may have altered and modified the expected results based on the preliminary investigations reported in Table 1. Since the proximate compositional analysis was performed with a significantly larger sample quantity, ~600–700 mg, the representativeness of the matrix can be considered higher in the latter case. Within this region, other thermally activated processes occurred without a noticeable loss of mass.

One process worth mentioning is the denaturation of proteins, wherein the application of thermal energy causes unfolding and subsequent alteration in protein structure [37,38].

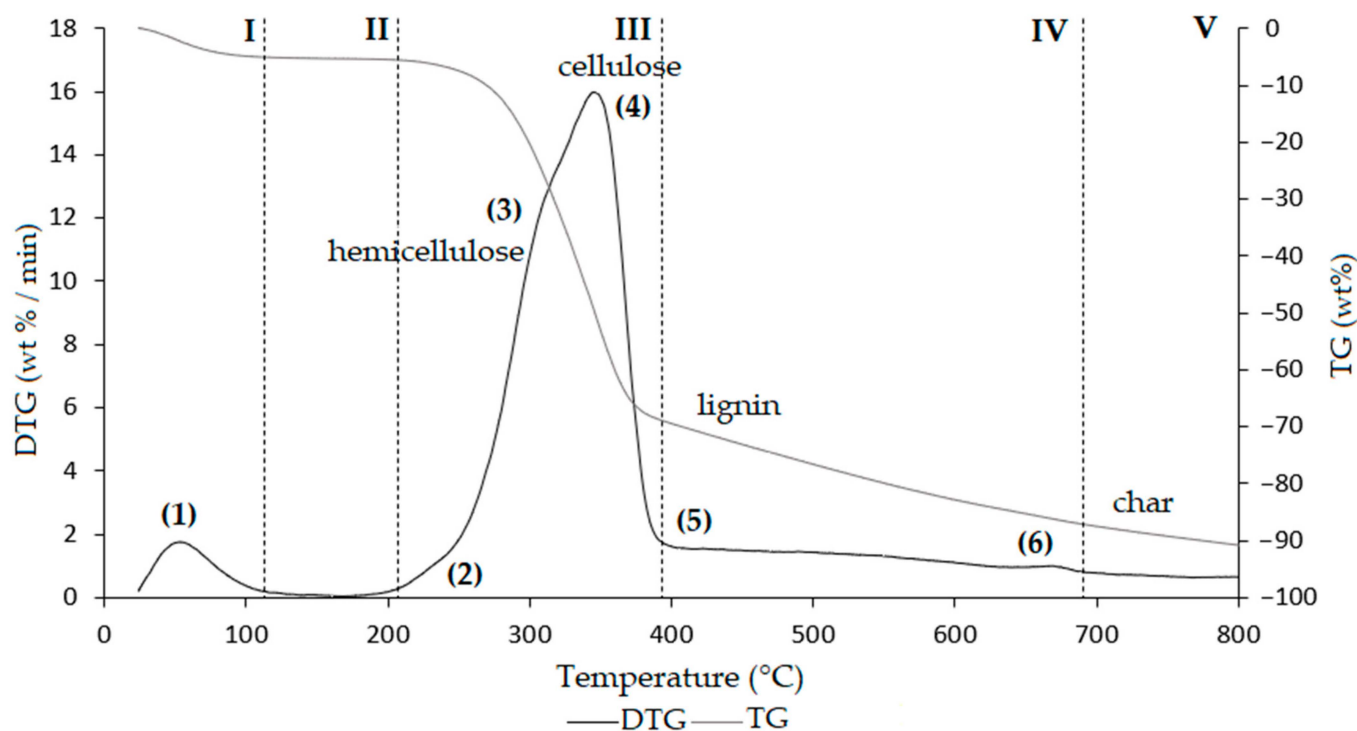


**Figure 2.** TG (grey line) and DTG (black line) curves of the Lambrusco Sorbara sample obtained at a heating rate of 20 °C/min under a He atmosphere. The vertical dashed lines indicate the five thermal regions (I–V) described in the text. Refer to Table 2 for the explanation of the numbers in parentheses.

Region II, covering the temperature range from ~120 °C to ~213 °C, primarily represents the mass loss attributed to bound water. This water mainly refers to the moisture retained by the inorganic fraction, such as the crystallization water of mineral salts. In this region, semi-volatile compounds with medium-low vapor pressure (SVOCs), which may be present in the initial matrix or formed during the heating phase, were completely removed ( $\Delta m\% = -2.0\%$ ). At approximately 160 °C, the removal of structural water begins, resulting from condensation reactions of the –OH groups primarily found in simple non-cellulosic carbohydrates [39]. At this temperature, significant modifications in the cellulose and hemicellulose fractions of the matrix were observed. Intermolecular water elimination through hydrogen bonds between two cellulose chains occurs, while hemicellulose dehydration is combined with the scission of weak linkages between small substituents and the main polymer chains [18]. The emission of volatile organic compounds associated with the degradation of cellulose and hemicellulose, examined in depth in Section 3.3, confirmed that these processes begin at approximately 160 °C. The formation and removal of reaction water traverses the entire thermogram up to and including Region IV. Furthermore, when the temperature reaches approximately 180 °C, thermal degradation processes start to affect free amino acids [40], whereas proteins retain their stability up to approximately 200–240 °C. Thus, the processes occurring in this region indicate the beginning of chemical structure destabilization, partial depolymerization, and plasticization of the biomass.

**Table 2.** Representative values of TGA/DTG profiles of Figure 2, obtained in inert atmosphere (He).

Region	Thermal Step	To	Tm	Tc	Δm%	Thermally Activated Processes
I	(1)	30	66	120	−3.3	Removal of moisture and VOCs up to 120 °C
II	(1)	120	–	213.5	−2.0	Removal of bound water, NH <sub>3</sub> from protein denaturation, low-boiling VOCs, loss of CO and CO <sub>2</sub>
III	(2)	213.5	–	240	−2.1	Shoulder related to protein degradation, removal of reaction water, NH <sub>3</sub> , low-boiling VOCs, and SVOCs, decarboxylation of acids with CO <sub>2</sub> loss, degradation of polysaccharides, plasticization, and pseudo-vitrification of the sample Fat degradation, removal of hydrocarbons, water of constitution, CO, and CO <sub>2</sub> , and volatilization of other metabolites
	(3)	240	297.9	318	−23.6	
	(4)	318	348.8	406.5	−37.3	
IV	(5)	406.5	–	641.3	−10.0	Removal of reaction water, CO <sub>2</sub> , and other metabolites, weak reactions related to slow volatilization of CO <sub>2</sub>
	(6)	641.3	658.7	680	−1.0	
V		680	–	800	−2.4	Volatilization of carbon residues, probably C <sub>20</sub> –C <sub>40</sub> fragments
		Residual ashes at 1000 °C				Inorganic compounds and carbon residue

To = onset temperature (beginning of thermal step processes); Tm = maximum temperature for the largest mass loss rate; Tc = conclusion temperature (end of thermal step processes).

Region III, occurring in the temperature range of  $\sim 213$  °C to  $\sim 406$  °C, represents the main pyrolysis window where structural decay reactions of proteins ( $\sim 240$  °C), hemicellulose ( $\sim 300$  °C) [20,41], and cellulose ( $\sim 370$  °C) [20,42] are observed. These reactions involve the breakdown of complex molecular structures, resulting in the release of volatile compounds and the formation of charred residues. The mass loss in this region was approximately  $\Delta m\% = -63.0\%$ , indicating substantial decomposition and transformation of the matrix.

In Region IV, which begins at  $\sim 406$  and extends up to  $\sim 680$  °C, the gradual decrease in mass is predominantly driven by the slow pyrolysis of the lignin fraction. This process is characterized by vitrification of the sample and the volatilization of carbon microparticles. However, the degradation of lignin occurs over a wide thermal range, from 150 to over 500 °C [43]. The high three-dimensional complexity of lignin contributes to this phenomenon, as specific fragments within its structure break down at different temperatures depending on the composition and type of lignin. The constituent units of lignin vary in their composition and possess different levels of thermal stability [19]. The small thermal event near 660 °C can be attributed to the thermal decomposition of the carbonaceous matter (biochar). Although this thermal event is mostly linked to the hemicellulose fraction [44], it is worth noting that lignin components may also contribute to its formation [45].

In Region V, above 680 °C, the last residue of biomass degradation was observed. This phase represents the typical carbon pyrolysis window, characterized by the thermal decomposition of low volatile matter, such as carbon fragments C20-C40. This stage involves the breakdown of carbon structures and the release of non-volatile carbonaceous materials, which, along with mineral ash, contribute to the formation of charred residue.

Emitted gases analysis (EGA) enables a more comprehensive understanding of the processes occurring during the thermal ramp. In particular, the evolutions of H<sub>2</sub>O, CO<sub>2</sub>, furfural, and acetic acid were investigated. Acetic acid is a distinctive indicator of hemicellulose degradation, whereas furfural is a distinctive indicator of both hemicellulose and cellulose loss [18,20]. Studying their changes provides valuable insights into the thermal degradation of our samples. Figure 3 shows the evolution trends of H<sub>2</sub>O ( $m/z = 18$ ), CO<sub>2</sub> ( $m/z = 44$ ), furfural (its fragment C<sub>3</sub>H<sub>3</sub><sup>+</sup> with  $m/z = 39$ ), and acetic acid ( $m/z = 60$ ) during the heating of the Lambrusco Sorbara sample. The EGA curves of qualitative interest for the four selected species are represented on the TIC scale relating to each activated channel for each of the same four analytes.

The evolutionary curve of H<sub>2</sub>O ( $m/z = 18$ ) is particularly interesting as it spans the entire thermogram until it reaches the baseline at approximately 700 °C. At lower temperatures, molecular water naturally present in the initial matrix was eliminated, with a gradual decrease in the signal until 210 °C. Beyond this threshold, the curve swiftly gains a thermal peak centered at approximately 320 °C, indicating the removal of structural water from the proteins, hemicellulose, and cellulose. The structural water, stemming from condensation reactions among the -OH groups of the aforementioned macromolecules or the degradation of other molecular species, continues to develop, albeit to a diminishing extent, until 700–800 °C when it reaches the baseline and the slope of the curve is essentially nullified.

The evolution of CO<sub>2</sub> ( $m/z = 44$ ) covers the entire thermogram, starting at a temperature of approximately 160 °C. This is consistent with the observations reported in Table 2, as this trend includes the degradation of proteins, cellulose, hemicellulose, and lignin.

The release of acetic acid ( $m/z = 60$ ), the main by-product of hemicellulose degradation, occurred earlier than that of furfural [18]. Although furfural is also produced from hemicellulose, it is not the primary product of its degradation. Acetic acid is predominantly formed through the elimination of O-acetyl groups attached to the xylan backbone of hemicellulose, and this process occurs at lower temperatures. As a result, acetic acid was one of the initial compounds released during the thermal degradation of hemicellulose. In contrast, furfural ( $m/z = 39$ ) is produced by the depolymerization of hemicellulose, particularly affecting the later and terminal portions of the xylan chain. This depolymerization reaction occurs at higher temperatures than the formation of acetic acid. Furfural production primarily

occurs through the cleavage of cellulose bonds, involving direct rearrangement during the depolymerization process [20]. As shown in Table 2, this process follows the initial degradation of hemicellulose, which plays a secondary role in furfural formation. During cellulose cleavage, the release of glucose units provides the basis for the subsequent formation of furfural. The glucose units undergo a series of rearrangement reactions, including dehydration and condensation, leading to the conversion of glucose into furfural.

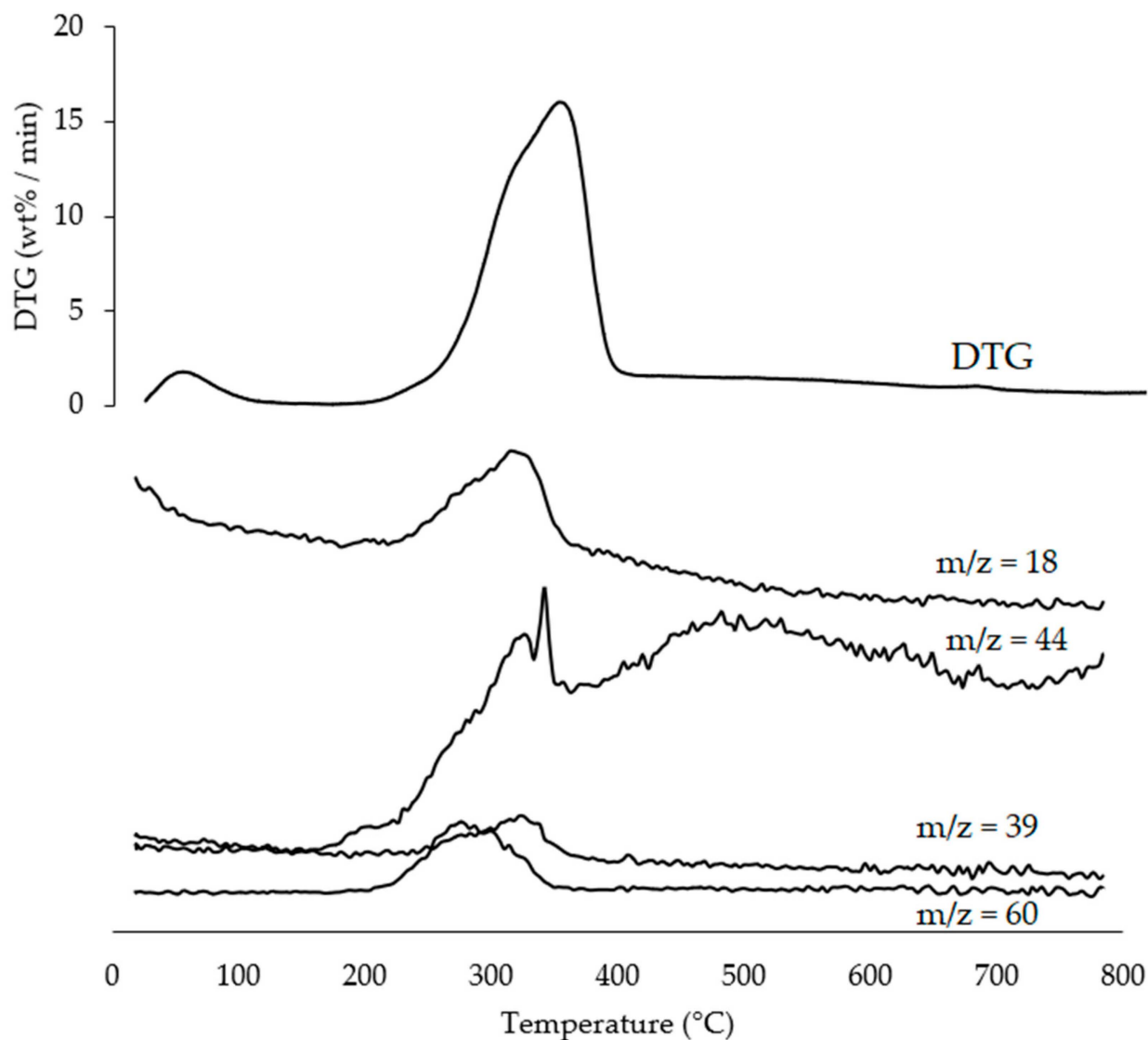


**Figure 3.** Evolution trend of H<sub>2</sub>O ( $m/z = 18$ ), CO<sub>2</sub> ( $m/z = 44$ ), furfural fragment C<sub>3</sub>H<sub>3</sub><sup>+</sup> ( $m/z = 39$ ), and acetic acid ( $m/z = 60$ ) during the heating of Lambrusco Sorbara wood sample; for ease of comparison, the DTG curve is also shown. Intensity of  $m/z$  is in arbitrary units.

### 3.3. HS-SPME-GC-MS

The results of the HS-SPME-GC-MS analysis are reported in Table 3. The compounds are listed divided by chemical class. The results are expressed as the mean of the TIC area ( $\times 10^6$ )  $\pm$  standard deviation (SD) of three replicates.

**Table 3.** HS-SPME-GC-MS results of the Spergola chip and Lambrusco Sorbara chip samples roasted at different temperatures (120, 140, 160, 180, 200, 220, 240 °C); Total ion current (TIC) area values.

Analyte	ID #	Spergola Chips						
		SO120	SO140	SO160	SO180	SO200	SO220	SO240
					TIC Area × 10 <sup>6</sup>			
					Aldehydes			
Propanal	A, B	-	0.126 ± 0.051 a	0.136 ± 0.090 a	0.327 ± 0.079 ab	0.523 ± 0.103 bc	0.752 ± 0.078 c	1.15 ± 0.11 d
Propanal, 2-methyl-	A, B, C	-	0.375 ± 0.054 a	0.230 *ab	0.111 ± 0.059 b	0.158 ± 0.096 ab	0.277 ± 0.065 ab	2.65 ± 0.15 c
Butanal, 3-methyl-	A, B	0.294 ± 0.086 a	0.291 ± 0.069 a	0.326 ± 0.098 a	0.396 ± 0.075 ab	0.488 ± 0.107 ab	0.688 ± 0.115 b	1.79 ± 0.19 c
Butanal, 2-methyl-	A, B	0.346 ± 0.079 a	0.321 *a	0.390 ± 0.058 a	0.463 ± 0.066 a	0.512 ± 0.077 a	0.956 ± 0.099 b	3.82 ± 0.20 c
Pentanal	A, B	0.241 *a	0.500 ± 0.124 b	0.793 ± 0.107 c	1.11 ± 0.13 d	0.317 ± 0.051 ab	0.296 ± 0.061 ab	0.191 *a
Hexanal	A, B, C	1.84 ± 0.17 a	2.09 ± 0.23 a	3.79 ± 0.14 b	5.36 ± 0.24 c	0.138 ± 0.096 d	0.128 ± 0.055 d	0.115 *d
Heptanal	A, B	-	0.130 *a	0.478 ± 0.056 b	0.646 ± 0.095 b	0.185 *a	0.102 ± 0.067 a	-
Octanal	A, B	0.079 *a	0.132 ± 0.086 a	0.577 ± 0.086 b	0.585 ± 0.093 b	0.155 ± 0.060 a	-	-
Nonanal	A, B, C	0.272 ± 0.059 a	0.304 ± 0.079 a	0.818 ± 0.105 b	0.640 ± 0.071 b	0.115 ± 0.098 a	-	-
					Esters			
Acetic acid, methyl ester	A, B, C	-	0.566 ± 0.099 a	2.06 ± 0.24 b	2.98 ± 0.30 c	5.55 ± 0.14 d	10.8 ± 0.1 e	38.8 ± 0.3 f
					Ketones			
Acetone	A, B, C	-	0.674 ± 0.079 a	1.29 ± 0.12 b	1.53 ± 0.09 bc	1.90 ± 0.18 c	2.42 ± 0.20 d	3.79 ± 0.15 e
2,3-Butanedione	A, B	0.182 ± 0.052 a	0.330 ± 0.103 a	0.847 ± 0.068 b	0.857 ± 0.080 b	1.35 ± 0.14 c	2.41 ± 0.11 d	4.63 ± 0.32 e
2-Butanone	A, B, C	-	-	-	-	0.441 ± 0.050 a	1.46 ± 0.16 b	5.14 ± 0.28 c
2,3-Pentanedione	A, B	-	-	-	0.236 *a	0.336 ± 0.057 a	0.845 ± 0.069 b	1.00 ± 0.12 b
2-Heptanone	A, B	-	-	0.165 ± 0.061 a	0.186 *a	0.210 *a	-	-
2-Cyclopenten-1-one, 2-methyl-	A, B	-	-	-	-	0.102 ± 0.053 a	0.367 ± 0.054 b	0.504 *c
Butyrolactone	A, B, C	-	-	-	-	0.124 *a	0.367 ± 0.080 b	0.504 ± 0.052 b
					Furan Derivatives			
Furan	A, B	-	-	-	-	2.04 ± 0.11 a	5.66 ± 0.25 b	13.7 ± 0.2 c
Furan, 2-methyl-	A, B	-	0.148 *a	0.245 ± 0.058 ab	0.184 ± 0.051 a	0.589 ± 0.078 b	2.79 ± 0.16 c	17.3 ± 0.3 d
Furan, 3-methyl-	A, B	-	-	-	-	0.103 *a	0.284 ± 0.066 a	1.14 ± 0.11 b
Furan, 2-ethyl-	A, B	0.118 *a	0.154 *a	0.339 ± 0.057 b	0.619 ± 0.051 c	0.633 ± 0.079 c	0.783 ± 0.064 cd	0.894 ± 0.095 d
Furan, 2,5-dimethyl-	A, B	-	-	-	-	0.073 *a	0.372 ± 0.053 a	1.52 ± 0.32 b
Furan, 2,4-dimethyl-	A, B	-	-	-	-	0.099 *a	0.195 *a	0.770 ± 0.084 b
2-Vinylfuran	A, B	-	-	-	-	0.099 *a	0.180 *ab	0.266 ± 0.061 b
3(2H)-Furanone, dihydro-2-methyl-	A, B	-	0.809 ± 0.099 a	1.40 ± 0.13 b	0.753 ± 0.085 a	0.421 ± 0.059 c	-	-
Furan, 2-ethyl-5-methyl-	A, B	-	-	-	-	-	0.100 *a	0.291 ± 0.062 b
Furfural	A, B, C	-	-	0.847 ± 0.086 a	0.365 ± 0.071 a	0.887 ± 0.074 a	3.02 ± 0.17 b	4.70 ± 0.34 b
Furan, 2-pentyl-	A, B	1.58 ± 0.15 a	0.969 ± 0.096 b	1.73 ± 0.11 a	1.87 ± 0.27 a	2.01 ± 0.21 a	1.66 ± 0.17 a	0.865 ± 0.054 b
					Organic Acids			
Acetic acid	A, B, C	4.77 ± 0.31 ab	4.64 ± 0.22 a	5.46 ± 0.10 b	7.45 ± 0.41 c	9.02 ± 0.37 d	21.1 ± 0.3 e	27.9 ± 0.2 f

Table 3. Cont.

Analyte	ID #	Spergola Chips						
		TIC Area × 10 <sup>6</sup>						
		Aromatic Compounds						
Benzene	A, B, C	-	-	-	-	-	0.180 ± 0.096 a	1.37 ± 0.17 b
1H-Pyrrole, 1-methyl-	A, B	-	-	-	-	0.102 *a	0.212 *b	0.435 ± 0.058 c
Toluene	A, B	-	-	-	-	0.228 ± 0.054 a	0.320 ± 0.055 a	0.761 ± 0.066 b
Benzyl alcohol	A, B	-	-	-	-	-	0.103 *a	0.343 *b
Benzene, 1,3-dimethyl-	A, B	-	-	-	-	0.269 ± 0.065 a	0.254 ± 0.067 a	0.247 ± 0.071 a
p-Xylene	A, B	-	-	-	-	0.189 ± 0.051 a	0.190 *a	0.177 *a
Phenol	A, B, C	-	-	-	-	0.291 *a	0.364 ± 0.062 ab	0.478 ± 0.068 b
Benzaldehyde	A, B	-	-	0.441 ± 0.058 a	0.593 ± 0.073 ab	0.665 ± 0.070 bc	0.836 ± 0.092 cd	0.945 ± 0.052 d
Guaiacol	A, B, C	-	-	-	0.360 ± 0.052 a	0.758 ± 0.086 b	0.954 ± 0.057 b	2.22 ± 0.28 c
Vanillin	A, B	-	-	-	0.102 *a	0.493 ± 0.063 b	0.997 ± 0.086 c	1.84 ± 0.18 d
		Terpenes						
Limonene	A, B, C	0.128 *a	0.079 *a	-	-	-	-	-
α-Copaene	A, B	0.859 ± 0.078 a	0.537 ± 0.067 b	0.304 ± 0.061 c	0.226 ± 0.054 c	-	-	-
Epizonarene	A, B	0.404 ± 0.052	-	-	-	-	-	-
γ-Cadinene	A, B	0.884 ± 0.058 a	0.415 ± 0.068 b	0.193 ± 0.051 c	0.156 *c	-	-	-
Calamenene	A, B	0.392 *	-	-	-	-	-	-
		Lambrusco Sorbara Chips						
Analyte	ID #	TIC Area × 10 <sup>6</sup>						
		SP120	SP140	SP160	SP180 Aldehydes	SP200	SP220	SP240
Propanal, 2-methyl-	A, B, C	4.38 ± 0.15 a	2.47 ± 0.28 b	11.0 ± 0.3 c	1.77 ± 0.21 d	3.54 ± 0.30 e	1.24 ± 0.12 d	6.02 ± 0.23 f
Butanal, 3-methyl-	A, B	2.42 ± 0.18 ac	1.11 ± 0.14 b	1.84 ± 0.11 ab	1.95 ± 0.18 a	3.13 ± 0.13 c	1.93 ± 0.08 ab	12.7 ± 0.7 d
Butanal, 2-methyl-	A, B	2.17 ± 0.30 a	1.98 ± 0.09 a	6.13 ± 0.32 b	4.79 ± 0.051 c	3.81 ± 0.17 d	3.63 ± 0.14 d	9.23 ± 0.20 e
Pentanal	A, B	-	2.94 ± 0.12 a	2.37 ± 0.20 b	2.35 ± 0.11 b	1.62 ± 0.15 c	0.792 ± 0.051 d	1.20 ± 0.09 e
Hexanal	A, B, C	3.32 ± 0.27 a	8.69 ± 0.35 b	6.21 ± 0.24 c	5.28 ± 0.17 d	4.86 ± 0.19 d	1.99 ± 0.10 e	-
Heptanal	A, B	-	0.443 ± 0.091 a	0.374 ± 0.066 ab	0.262 *b	-	-	-
Octanal	A, B	-	0.305 ± 0.088 a	0.230 *a	0.240 ± 0.051 a	-	-	-
Nonanal	A, B, C	-	0.968 ± 0.107 a	0.163 *b	0.221 *b	-	-	-
		Esters						
Methyl formate	A, B	0.393 ± 0.052 a	0.309 ± 0.064 a	2.56 ± 0.15 b	3.49 ± 0.23 c	10.4 ± 0.3 d	7.35 ± 0.13 e	6.19 ± 0.20 f
Acetic acid, methyl ester	A, B, C	0.981 ± 0.098 a	2.13 ± 0.11 a	12.0 ± 0.4 b	16.5 ± 0.3 c	68.1 ± 1.7 d	76.4 ± 1.9 e	116 ± 1 f
Propanoic acid, methyl ester	A, B	-	-	-	0.319 ± 0.063 a	1.56 ± 0.23 b	2.53 ± 0.16 c	3.98 ± 0.21 d

Table 3. Cont.

Analyte	ID #	Spergola Chips			TIC Area × 10 <sup>6</sup>			
					Ketones			
Acetone	A, B, C	1.83 ± 0.23 a	4.12 ± 0.11 b	7.64 ± 0.20 c	5.63 ± 0.14 d	13.4 ± 0.9 e	12.9 ± 0.4 e	16.9 ± 0.2 f
2,3-Butanedione	A, B	0.895 ± 0.066 a	1.10 ± 0.20 a	4.46 ± 0.17 b	3.26 ± 0.24 b	16.1 ± 1.1 c	16.4 ± 0.9 c	25.5 ± 0.3 d
2-Butanone	A, B, C	0.251 ± 0.059 a	0.357 ± 0.063 a	1.43 ± 0.09 b	1.52 ± 0.10 b	4.96 ± 0.17 c	6.48 ± 0.11 d	11.7 ± 0.1 e
2-Propanone, 1-hydroxy-	A, B	-	-	0.634 ± 0.075 a	1.00 ± 0.08 a	1.45 ± 0.09 b	1.48 ± 0.10 b	5.79 ± 0.31 c
2,3-Pentanedione	A, B	-	-	1.60 ± 0.15 a	1.15 ± 0.16 a	3.38 ± 0.22 b	2.77 ± 0.14 c	9.38 ± 0.29 d
2-Butanone, 3-hydroxy-	A, B	-	-	0.474 ± 0.057 a	0.210 <sup>a</sup> a	3.61 ± 0.11 b	0.264 ± 0.058 a	5.96 ± 0.32 c
2-Heptanone	A, B	-	0.107 ± 0.071 a	0.289 <sup>b</sup> b	0.299 ± 0.051 b	-	-	-
2-Cyclopenten-1-one, 2-methyl-	A, B	-	-	-	-	-	0.152 <sup>a</sup> a	0.963 ± 0.085 b
Butyrolactone	A, B, C	-	-	0.317 ± 0.059 a	0.402 ± 0.065 a	1.35 ± 0.08 b	1.50 ± 0.13 b	4.92 ± 0.14 c
					Furan Derivatives			
Furan	A, B	-	-	-	-	65.1 ± 3.4 a	72.0 ± 2.0 b	72.7 ± 1.7 b
Furan, 2-methyl-	A, B	0.418 ± 0.089 a	0.477 ± 0.057 a	2.53 ± 0.17 b	2.58 ± 0.13 b	19.9 ± 0.4 c	15.0 ± 0.3 d	48.9 ± 0.7 e
Furan, 3-methyl-	A, B	-	-	-	0.143 <sup>a</sup> a	1.42 ± 0.07 b	1.15 ± 0.09 b	4.04 ± 0.16 c
Furan, 2-ethyl-	A, B	-	1.54 ± 0.16 a	1.07 ± 0.09 b	0.608 ± 0.050 c	2.38 ± 0.09 d	2.34 ± 0.05 d	2.32 ± 0.07 d
Furan, 2,5-dimethyl-	A, B	-	-	-	0.161 <sup>a</sup> a	1.43 ± 0.10 b	1.65 ± 0.10 b	4.23 ± 0.19 c
3(2H)-Furanone, dihydro-2-methyl-	A, B	-	0.194 ± 0.059 a	1.12 ± 0.10 b	0.999 ± 0.064 b	2.89 ± 0.14 c	0.953 ± 0.076 b	1.13 ± 0.12 b
Furfural	A, B, C	-	-	1.10 ± 0.08 a	6.42 ± 0.42 b	21.9 ± 0.9 c	24.1 ± 1.0 d	44.9 ± 0.7 e
2-Furanmethanol	A, B	-	-	-	-	-	0.869 ± 0.067 a	4.77 ± 0.13 b
2-Furancarboxyaldehyde, 5-methyl-	A, B, C	-	-	-	0.357 ± 0.071 a	3.21 ± 0.27 b	3.63 ± 0.30 b	4.39 ± 0.22 c
3-Furancarboxylic acid, methyl ester	A, B	-	-	-	-	-	-	1.03 ± 0.07
2-Furanmethanol, acetate	A, B	-	-	-	-	-	0.393 ± 0.056 a	2.05 ± 0.13 b
Furan, 2-pentyl-	A, B	2.81 ± 0.23 a	4.06 ± 0.17 b	4.16 ± 0.23 b	0.465 ± 0.074 c	0.945 ± 0.096 c	-	-
					Organic Acids			
Acetic acid	A, B, C	4.73 ± 0.22 a	24.9 ± 0.3 b	25.0 ± 0.4 b	33.7 ± 0.7 c	53.5 ± 1.3 d	80.4 ± 2.3 e	96.6 ± 4.1 f
Propanoic acid	A, B	-	-	-	-	-	0.456 ± 0.083 a	5.47 ± 0.21 b
					Aromatic Compounds			
Benzene	A, B, C	-	-	-	0.397 ± 0.061 a	0.424 ± 0.051 a	-	-
3-Methylpyridazine	A, B	-	-	-	-	-	0.587 ± 0.067 a	1.37 ± 0.21 b
1H-Pyrrole, 1-methyl-	A, B	-	-	-	-	0.270 ± 0.062 a	0.391 <sup>a</sup> a	1.42 ± 0.11 b
Pyridine	A, B	-	-	-	-	-	0.522 ± 0.068 a	2.31 ± 0.13 b
Toluene	A, B	-	-	-	0.399 <sup>a</sup> a	0.828 ± 0.077 b	0.454 ± 0.061 a	2.23 ± 0.30 c
p-Xylene	A, B	-	-	-	0.762 ± 0.051 a	0.851 ± 0.071 a	0.191 <sup>b</sup> b	-
Phenol	A, B, C	-	-	-	-	-	0.412 ± 0.079 a	0.711 ± 0.069 b
Benzaldehyde	A, B	0.379 ± 0.065 a	0.400 ± 0.077 a	0.553 ± 0.050 a	0.505 ± 0.063 a	0.663 ± 0.080 b	-	-
Guaiacol	A, B, C	-	-	-	0.460 ± 0.052 a	0.846 ± 0.066 ab	1.07 ± 0.12 b	4.85 ± 0.26 c
Guaiacol, 4-methyl-	A, B	-	-	-	-	-	-	0.161 <sup>*</sup> *
Syringol	A, B	-	-	-	-	-	-	0.188 <sup>*</sup> *
Vanillin	A, B	-	-	-	0.160 <sup>a</sup> a	0.563 ± 0.063 b	0.697 ± 0.071 b	1.21 ± 0.17 c

**Table 3.** *Cont.*

Analyte	ID #	Spergola Chips			TIC Area × 10 <sup>6</sup>			
					Terpenes			
Ylangene	A, B	0.460 ± 0.051 a	0.323 *b	-	-	-	-	-
					Sulfur Compounds			
Thiophene	A, B	-	-	-	-	-	-	0.765 ± 0.062
Disulfide, dimethyl-	A, B	-	0.131 *a	0.199 *a	0.425 ± 0.088 a	2.15 ± 0.11 b	2.40 ± 0.25 b	5.03 ± 0.20 c
Trisulfide, dimethyl-	A, B	-	-	-	-	-	-	0.549 ± 0.074

Data are expressed as mean ± standard deviation (SD) of three replicates; \* SD < 0.05. # The identification of the compounds was obtained via: (A) the mass spectral data of the libraries supplied with the operating system of the GC-MS and from mass spectra databases; (B) the mass spectra found in the literature; and (C) the mass spectra and retention time of an injected standard. Differences among means indicated by the same letters are not statistically significant ( $p < 0.05$ ) using Tukey–Kramer HSD post hoc test.

In Table 3, it can be observed that the compounds identified in the Lambrusco Sorbara and Spergola grapevine chips consisted of aldehydes, esters, ketones, furan derivatives, organic acids, aromatic compounds, and terpenes. One notable difference was the presence of three sulfur compounds, thiophene, dimethyl disulfide, and dimethyl trisulfide, in the Spergola grapevine chip samples, which were not detected in the Sorbara samples.

The main differences in the VOC composition of the samples are summarized in Table 4. This table presents the cumulative TIC area of individual analytes grouped by chemical class, offering insights into the compositional differences between the two cultivars and the variations resulting from different roasting temperatures. One-way analysis of variance (ANOVA) was performed to assess whether there were statistically significant differences among the quantities of each compound class of the roasted grapevine samples. For each roasting temperature, a two-sample *t*-test (with a significance level of  $p < 0.05$ ) was conducted to identify significant differences between the two cultivars. The *p*-value for all investigated compound classes was smaller than the significance level (0.05). Therefore, we can conclude that, globally, the investigated grapevine chip samples were statistically different.

**Table 4.** HS-SPME-GC-MS results of the Sorbara (SO) and Spergola (SP) roasted chip samples.

	TIC Area × 10 <sup>6</sup>							
	ALD	EST	KET	FUD	OA	ARC	TER	SUL
SO120	3.07 ± 0.39 a	-	0.182 ± 0.052 a	1.70 ± 0.15 a	4.77 ± 0.31 a	-	2.67 ± 0.19 a	-
SO140	4.27 ± 1.40 a	0.566 ± 0.099 a	0.330 ± 0.182 a	2.08 ± 0.19 a	4.64 ± 0.22 a	-	1.03 ± 0.13 b	-
SO160	7.54 ± 0.74 b	2.06 ± 0.24 b	1.01 ± 0.25 a	4.56 ± 0.44 b	5.46 ± 0.10 a	0.441 ± 0.058 a	0.498 ± 0.112 c	-
SO180	9.64 ± 0.91 b	2.98 ± 0.30 c	1.28 ± 0.17 ab	3.79 ± 0.53 ab	7.45 ± 0.41 b	2.92 ± 0.12 b	0.381 ± 0.054 c	-
SO200	2.59 ± 0.69 a	5.55 ± 0.14 d	2.56 ± 0.48 b	6.96 ± 0.61 c	9.02 ± 0.37 c	3.00 ± 0.39 b	-	-
SO220	3.20 ± 0.54 a	10.8 ± 0.1 e	5.31 ± 0.67 c	15.0 ± 0.9 d	21.1 ± 0.3 d	4.41 ± 0.51 c	-	-
SO240	9.72 ± 0.65 b	38.8 ± 0.3 f	11.8 ± 0.9 d	41.5 ± 1.6 e	27.9 ± 0.2 e	6.98 ± 0.94 d	-	-
SP120	12.3 ± 0.9 a	1.37 ± 0.15 a	2.98 ± 0.35 a	3.23 ± 0.32 a	4.73 ± 0.22 a	0.379 ± 0.065 a	0.460 ± 0.051 a	-
SP140	18.9 ± 1.3 b	2.44 ± 0.17 b	5.68 ± 0.44 a	6.26 ± 0.45 ab	24.9 ± 0.3 b	0.400 ± 0.077 a	0.323 *b	0.131 *a
SP160	28.3 ± 1.2 c	14.6 ± 0.5 c	16.8 ± 0.8 b	9.98 ± 0.67 ab	25.0 ± 0.4 b	0.553 ± 0.050 a	-	0.199 *a
SP180	16.9 ± 0.8 b	20.3 ± 0.6 d	13.5 ± 0.8 b	11.7 ± 0.8 b	33.7 ± 0.7 c	2.68 ± 0.23 b	-	0.425 *a
SP200	16.9 ± 0.9 b	80.1 ± 2.2 e	44.2 ± 2.7 c	119 ± 5 c	53.5 ± 1.3 d	4.45 ± 0.47 c	-	2.15 ± 0.09 b
SP220	9.58 ± 0.49 a	86.3 ± 2.2 f	42.0 ± 1.8 c	122 ± 4 c	80.8 ± 2.8 e	9.61 ± 0.47 d	-	2.40 ± 0.11 b
SP240	29.2 ± 1.2 c	126 ± 1 g	81.2 ± 1.7 d	191 ± 4 d	102 ± 4 f	14.4 ± 1.2 e	-	6.35 ± 0.34 c

Data are expressed as mean ± standard deviation (SD) of three replicates; \* SD < 0.05; ALD = aldehydes; EST = esters; KET = ketones; FUD = furan derivatives; OA = organic acids; ARC = aromatic compounds; TER = terpenes; SUL = sulfur compounds; differences among means indicated by the same letters are not statistically significant ( $p < 0.05$ ) using Tukey–Kramer HSD post hoc test.

From Table 4, it is evident that the chromatogram of the Spergola cultivar samples displayed significantly higher total ion current (TIC) areas than those of Sorbara. For example, the cumulative areas of individual peaks corresponding to the SO240 and SP240 samples were  $1.37 \times 10^8$  and  $5.50 \times 10^8$ , respectively. This indicates that the Spergola cultivar samples had a more intense and noticeable aroma.

The aldehyde content followed a similar pattern in both cultivars. A gradual increase was observed up to a roasting temperature of 160 °C for the Sorbara samples and 180 °C for the Spergola samples, followed by a significant decrease up to 220 °C. Subsequently, from 220 to 240 °C, there was a strong increase in the aldehyde content. The trend in the concentration of aldehydes, such as hexanal, heptanal, and octanal, clarifies the declines observed at 160 °C and 180 °C. Specifically, these aldehydes exhibited a progressive increase in concentration up to these temperatures, followed by a sharp decrease. Hexanal, heptanal, and octanal are well-known byproducts of lipid oxidation. Despite the low lipid content in grapevine wood [46], even trace amounts can serve as precursors for the generation of these aldehydes through oxidative breakdown. The noteworthy decrease in the TIC area observed after reaching 180 °C can be explained by their volatilization and lipid depletion. On the other hand, other aldehydes, such as 2- and 3-methylbutanal and 2-methylpropanal, showed a progressive increase in concentration as the roasting temperature increased, with the maximum variation occurring between 220 °C and 240 °C. These aldehydes mainly contributed to the overall increase observed in the entire class of aldehydes during this thermal step. 2-methylbutanal, 3-methylbutanal, and 2-methylpropanal are commonly

referred to as Strecker aldehydes [47]. They are frequently detected in the low-boiling fraction of volatile compounds in processed plant foods [14,16]. Their presence indicates that the Maillard reaction occurred during the roasting process of the grapevine chip samples [47]. Strecker aldehydes are known for their low odor thresholds and are responsible for imparting cocoa, nutty, fruity, and fermented notes to the aroma profile [48].

The main ester detected in the samples of both cultivars was acetic acid methyl ester, also known as methyl acetate. Its concentration strongly increased with the roasting temperature in the samples of both cultivars, although the TIC area was significantly higher in the Spergola grapevine chips. Methyl acetate imparts fruity, wine, and whiskey-like notes to the aroma profile of the samples [49]. Its formation can be attributed to the reaction between acetic acid and methanol, which are the two main by-products of hemicellulose degradation. The concentration of acetic acid, the main organic acid identified in Sorbara and Spergola grapevine chips, also increased with the roasting temperature. This observation is in line with the findings of the TGA-MS-EGA (Section 3.2), which showed a progressive release of this volatile compound with the increasing temperature.

Ketones progressively increased with the roasting temperature, reaching the highest value in grapevine chips roasted at 240 °C.  $\alpha$ -Dicarbonyl compounds, such as 2,3-butanedione and 2,3-pentanedione, have low odor thresholds and are responsible for buttery and creamy notes in many cooked foods [50]. Lactones, such as butyrolactone, detected at temperatures above 160 °C in the SP samples and above 200 °C in the SO samples, also have low odor thresholds and are considered potent aroma compounds. Butyrolactone imparts creamy and fatty nuances and has been reported as a volatile aroma compound in other roasted wood samples [50].

The thermal degradation of wood polysaccharides leads to the formation of furanic derivatives, such as furfural, 5-methylfurfural, 2-furanmethanol, 2-methylfuran, and 3-methylfuran. These compounds arise when wood is subjected to heating; pentoses, which are the main constituents of hemicellulose, produce furfural, whereas 5-methylfurfural is formed from the hexose units, which are minor constituents of hemicelluloses and the main constituents of the more crystalline cellulose [18]. In this study, it was observed that the Spergola samples contained higher concentrations of furanic compounds compared to the Sorbara samples. Their presence strongly contributed to the overall aroma of the roasted grapevine chips, with the Spergola cultivar exhibiting a more pronounced sweet and toasted almond-like aroma. Furanic compounds are known for imparting sweet, nutty, and caramel-like characteristics to food [50]. Oxygenated furans, such as furfural, furfuryl alcohol, and 5-methylfurfural, contribute to the sweet, fruity, and caramel notes found in various cooked food products. 3(2H)-Furanone, dihydro-2-methyl-, which is commonly found in heated and non-heated foods, adds brown, sweet, rummy, and nut-like nuances to the overall aroma. It has been found in many studies regarding brown sugar aroma, together with butyrolactone [51].

Lignin, a complex polymer in wood, consists of two central structural units: guaiacyl and syringyl. While some studies have suggested that these structural units can begin to be released at temperatures around 150 °C [52,53], in our samples, we detected the resulting volatile compounds starting at a temperature of 180 °C. During the thermal treatment of lignocellulosic materials, such as grapevine wood, significant chemical transformations occur in the lignin component, leading to the formation of various degradation products. These degradation compounds contribute to the unique aroma profile associated with thermally treated wood and are known to impart sweet and spicy aromas [18]. In the case of grapevine chips, both cultivars emitted the lignin degradation compounds, guaiacol and vanillin. However, only the Spergola samples emitted additional compounds such as syringol and 4-methylguaiacol. All these compounds were detected starting at a roasting temperature of 180 °C, and their concentrations increased up to 240 °C. Vanillin is highly regarded as a flavor compound worldwide [50] and is known for its distinct sweet, creamy, and vanilla-like aroma. This significantly contributes to the desirable sensory qualities of thermally treated wood. Its characteristic scent enhances the overall aromatic attributes,

contributing to the perception of high-quality and well-roasted wood. In addition to its applications in the flavor and food sectors, vanillin exhibits various biological activities. Studies [54,55] have reported its antimicrobial effects on fungi, such as *Aspergillus flavus*, as well as bacteria, like *Escherichia coli* and *Staphylococcus aureus*, which make vanillin a potential food preservative for a wide variety of products. Considering the application of grapevine chips for aging alcoholic beverages and vinegars, the presence of vanillin could add value to the final product by contributing to its preservation and flavor profile. Additionally, vanillin has been investigated for its antioxidant, antimutagenic, anticlastogenic, and anticarcinogenic activities in several studies [56,57]. These health-promoting properties further enhance the appeal of vanillin as a valuable component of food and beverage products. Guaiacol is a phenolic compound that emits a smoky, vanillin, sweet aroma. It is formed through the cleavage of ether linkages in lignin, particularly from guaiacyl units. This adds complexity to the overall aroma profile and is an important contributor to the sensory experience of thermally treated wood products.

Sesquiterpenes are a class of volatile organic compounds that are commonly found in various plant species, including wood. They belong to the larger class of terpenes, which are organic compounds synthesized by plants via the mevalonate pathway [58]. Sesquiterpenes are characterized by their complex structures, consisting of 15 carbon atoms and their distinct aromas. In plants, sesquiterpenes serve multiple functions, including defense against herbivores, attraction of pollinators, and communication with neighboring organisms [58]. These compounds can act as chemical signals to deter herbivores or attract insects that are beneficial for pollination. Additionally, some sesquiterpenes exhibit antimicrobial and antioxidant properties, which further contribute to plant defense mechanisms [59]. Sesquiterpenes were identified only at temperatures up to 160 °C. Sesquiterpenes are relatively volatile and can undergo decomposition or evaporation at high temperatures, resulting in a decrease in their concentrations. Higher temperatures may accelerate the breakdown of sesquiterpenes into smaller compounds or cause their complete loss through evaporation. The formation and presence of specific sesquiterpenes in grapevine wood are influenced by the precursor compounds available in plant tissues. Different plant species, varieties, and even different parts of the same plant can contain varying amounts and types of sesquiterpene precursors [60]. The observed variations in sesquiterpene composition between the grapevine chip samples of the two cultivars suggest a genetic influence on the biosynthesis and accumulation of these compounds. The presence of specific sesquiterpenes in varying proportions in different grapevine cultivars imparts distinct aromatic notes, resulting in cultivar-specific olfactory profiles. This is an important aspect for aged beverages, since the unique sesquiterpene composition of each cultivar can influence their final sensory attributes if used as infused chips during the aging process. It can provide consumers with a diverse range of flavor experiences. The terpene content was higher in the Sorbara samples, both in terms of the number of analytes detected and the TIC area. We detected limonene,  $\alpha$ -copaene, epizonarene,  $\gamma$ -cadinene, and calamenene in the SO grapevine chips, while only ylangene was detected in the SP chips. They impart different aromatic notes, for example, limonene has sweet, orange, citrus, and terpenic notes, and  $\alpha$ -Copaene has woody, spicy, and honey notes, while ylangene is reported as a satisfactory marker for the 'pepper' aroma in grapes and wine [61].

Sulfur volatiles, which have been exclusively detected in Spergola grapevine chips, often play a crucial role in shaping the aroma of processed foods. Some studies [62,63] have identified different food products as rich sources of sulfur aroma compounds, with cysteine, methionine, and thiamine being particularly important precursors. The Maillard reaction is a key pathway for the formation of sulfur aroma compounds during cooking. Cysteine is the most important precursor of Maillard reaction-derived sulfur volatiles [64]. The differences in the presence of sulfur volatiles between the two grapevine cultivars likely stem from genotypic variations and differences in the amino acid composition of the grapevine wood.

Wood combustion is a well-known and significant contributor to air pollution, releasing various harmful pollutants, including benzene, xylene, and toluene [65]. These toxic compounds have chronic and detrimental impacts on both the environment and human health, leading to their classification as priority toxic pollutants. Benzene, a prevalent atmospheric contaminant, can originate from both natural sources like forest fires and volcanic activity, as well as human activities, such as cigarette smoking and the combustion of fossil fuels. The International Agency for Research on Cancer (IARC) [66,67] has classified benzene as a Group 1 human carcinogen, which is known to cause cancer in humans. Moreover, benzene can also form during cooking processes through the thermal decomposition of food components, and can be found in certain food additives, such as liquid smoke, which is derived from partial wood combustion [68]. Given that biomass combustion typically yields these compounds, the detection of benzene, xylene, and toluene in samples roasted at temperatures higher than 180 °C was not entirely unexpected. However, it is crucial to highlight that samples roasted at 200 °C exhibited significantly low TIC areas for these pollutants, with benzene, toluene, and xylene registering relative TIC areas of 0.13%, 0.25%, and 0.26%, respectively, in the Spergola cultivar, and 0%, 0.91%, and 0.88%, respectively, in the Sorbara cultivar. This suggests that the formation of toxic compounds was effectively mitigated at this temperature. However, it is essential to consider that as the temperature exceeds 200 °C, there is a possibility of increased generation of harmful molecules. This raises concerns about the suitability of grapevine chips roasted at temperatures higher than 200 °C for applications in the aging of alcoholic beverages. To ensure the safety and quality of the final product, it is advisable to adhere to roasting temperatures below this critical threshold. Further research is required to understand the exact mechanisms and kinetics of toxic compound formation during roasting. This knowledge could aid in developing optimized roasting conditions that minimize the production of harmful pollutants while preserving the desired aroma and flavor characteristics of grapevine chips for beverage aging.

The choice of roasting temperature for potential applications in the aging process of beverages is inherently multifaceted. Each beverage category possesses a distinct flavor profile, ranging from delicate to robust, and is influenced by a multitude of factors, including the base ingredients, fermentation process, and aging conditions. One important consideration when determining the roasting temperature is the characteristics and the nature of the beverage. Different beverages, such as wines, spirits, and vinegars, possess distinctive flavor profiles and aromatic nuances. For instance, wines may exhibit a wide range of flavors, from fruity and floral notes to woody and smoky undertones. On the other hand, spirits may feature intricate combinations of spices, herbs, and aging-derived flavors. In contrast, vinegars exhibit a spectrum of acidity levels and subtle fruity or oaky characteristics. The choice of roasting temperature should be aligned with the intended sensory enhancement objectives. Producers must consider whether they aim to emphasize specific flavor elements within their beverages, such as fruity or woody notes. In doing so, they could adjust the roasting temperature to accentuate the desired attributes. For example, a lower roasting temperature may be suitable for intensifying fruity and woody nuances, whereas a higher temperature could be preferred for highlighting smoky undertones.

#### 4. Conclusions

The findings of this study shed light on the remarkable potential of reusing grapevine wood, specifically roasted grapevine chips, as a sustainable and environmentally friendly alternative to incineration. By reusing grapevine wood, we can avoid contributing to pollution caused by incineration, thus promoting a more eco-conscious approach to waste management. Furthermore, aroma profile analysis revealed fascinating insights into the benefits of using roasted grapevine chips for the aging of alcoholic beverages and vinegars. The choice of grapevine cultivar and roasting temperature significantly affected the aroma profile of the chips, thereby offering unique and appealing sensory experiences. As the roasting temperature increased, the aroma profile became progressively enriched with

various aromatic compounds. Notably, lignin degradation products, such as guaiacol and vanillin have emerged, imparting smoky and sweet notes that are highly sought after and admired in aged beverages. The presence of furan derivatives, which contribute to the sweet, nutty, and caramel-like notes, further enhances the aromatic complexity and desirability of the final product. However, it is essential to exercise caution and limit the roasting temperature to 220 °C to prevent the formation of potentially harmful compounds, such as benzene and xylenes. Moreover, the identification of sesquiterpenes exclusively at temperatures up to 160 °C and their association with specific grapevine cultivars emphasize the influence of genotypic variations on the final aroma profile.

This study opens up exciting possibilities for the further exploration and application of roasted grapevine chips in the beverage industry, while fostering environmental responsibility and promoting a circular economy approach.

**Author Contributions:** Conceptualization, V.D.; methodology, V.D. and L.M.; software, V.D.; validation, V.D. and A.M.; formal analysis, A.M.; investigation, V.D. and L.M.; resources, A.M. and L.T.; data curation, L.M.; writing—original draft preparation, V.D.; writing—review and editing, L.M., L.T.; visualization, V.D.; supervision, A.M.; project administration, L.T.; funding acquisition, L.T. All authors have read and agreed to the published version of the manuscript.

**Funding:** This research received no external funding.

**Data Availability Statement:** The data are contained within the article.

**Conflicts of Interest:** The authors declare no conflict of interest.

## References

1. D'Eusanio, V.; Malferrari, D.; Marchetti, A.; Roncaglia, F.; Tassi, L. Waste By-Product of Grape Seed Oil Production: Chemical Characterization for Use as a Food and Feed Supplement. *Life* **2023**, *13*, 326. [CrossRef]
2. Albergamo, A.; Costa, R.; Bartolomeo, G.; Rando, R.; Vadalà, R.; Nava, V.; Gervasi, T.; Toscano, G.; Germanò, M.P.; D'Angelo, V.; et al. Grape Water: Reclaim and Valorization of a By-product from the Industrial Cryoconcentration of Grape (*Vitis vinifera*) Must. *J. Sci. Food Agric.* **2020**, *100*, 2971–2981. [CrossRef] [PubMed]
3. OIV. State of the World Vine and Wine Sector 2021. Available online: [https://www.oiv.int/sites/default/files/documents/eng-state-of-the-world-vine-and-wine-sector-april-2022-v6\\_0.pdf](https://www.oiv.int/sites/default/files/documents/eng-state-of-the-world-vine-and-wine-sector-april-2022-v6_0.pdf) (accessed on 10 April 2023).
4. Famiyeh, L.; Chen, K.; Xu, J.; Sun, Y.; Guo, Q.; Wang, C.; Lv, J.; Tang, Y.-T.; Yu, H.; Snape, C.; et al. A Review on Analysis Methods, Source Identification, and Cancer Risk Evaluation of Atmospheric Polycyclic Aromatic Hydrocarbons. *Sci. Total Environ.* **2021**, *789*, 147741. [CrossRef] [PubMed]
5. Ogawa, M.; Yoshida, N. Nitrous Oxide Emission from the Burning of Agricultural Residue. *Atmos. Environ.* **2005**, *39*, 3421–3429. [CrossRef]
6. D'Eusanio, V.; Genua, F.; Marchetti, A.; Morelli, L.; Tassi, L. Characterization of Some Stilbenoids Extracted from Two Cultivars of Lambrusco—*Vitis Vinifera* Species: An Opportunity to Valorize Pruning Canes for a More Sustainable Viticulture. *Molecules* **2023**, *28*, 4074. [CrossRef]
7. Lambert, C.; Richard, T.; Renouf, E.; Bisson, J.; Waffo-Téguo, P.; Bordenave, L.; Ollat, N.; Mérillon, J.-M.; Cluzet, S. Comparative Analyses of Stilbenoids in Canes of Major *Vitis Vinifera* L. Cultivars. *J. Agric. Food Chem.* **2013**, *61*, 11392–11399. [CrossRef]
8. Rivière, C.; Pawlus, A.D.; Mérillon, J.-M. Natural Stilbenoids: Distribution in the Plant Kingdom and Chemotaxonomic Interest in Vitaceae. *Nat. Prod. Rep.* **2012**, *29*, 1317. [CrossRef]
9. Athar, M.; Back, J.; Tang, X.; Kim, K.; Kopelovich, L.; Bickers, D.; Kim, A. Resveratrol: A Review of Preclinical Studies for Human Cancer Prevention. *Toxicol. Appl. Pharmacol.* **2007**, *224*, 274–283. [CrossRef]
10. Gómez-Zorita, S.; Milton-Laskibar, I.; Eseberri, I.; Beaumont, P.; Courtois, A.; Krisa, S.; Portillo, M.P. Beneficial Effects of  $\epsilon$ -Viniferin on Obesity and Related Health Alterations. *Nutrients* **2023**, *15*, 928. [CrossRef]
11. Chang, X.; Heene, E.; Qiao, F.; Nick, P. The Phytoalexin Resveratrol Regulates the Initiation of Hypersensitive Cell Death in *Vitis* Cell. *PLoS ONE* **2011**, *6*, e26405. [CrossRef]
12. Sánchez-Gómez, R.; Zalacain, A.; Alonso, G.L.; Salinas, M.R. Vine-Shoot Waste Aqueous Extracts for Re-Use in Agriculture Obtained by Different Extraction Techniques: Phenolic, Volatile, and Mineral Compounds. *J. Agric. Food Chem.* **2014**, *62*, 10861–10872. [CrossRef] [PubMed]
13. UN General Assembly. *Transforming Our World: The 2030 Agenda for Sustainable Development*; A/RES/70/1; United Nations: Nairobi, Kenya, 2015.
14. D'Eusanio, V.; Maletti, L.; Marchetti, A.; Roncaglia, F.; Tassi, L. Volatile Aroma Compounds of Gavina<sup>®</sup> Watermelon (*Citrullus Lanatus* L.) Dietary Fibers to Increase Food Sustainability. *AppliedChem* **2023**, *3*, 66–88. [CrossRef]

15. Maletti, L.; D'Eusanio, V.; Durante, C.; Marchetti, A.; Pincelli, L.; Tassi, L. Comparative Analysis of VOCs from Winter Melon Pomace Fibers before and after Bleaching Treatment with H<sub>2</sub>O<sub>2</sub>. *Molecules* **2022**, *27*, 2336. [CrossRef] [PubMed]
16. Maletti, L.; D'Eusanio, V.; Durante, C.; Marchetti, A.; Tassi, L. VOCs Analysis of Three Different Cultivars of Watermelon (*Citrullus Lanatus* L.) Whole Dietary Fiber. *Molecules* **2022**, *27*, 8747. [CrossRef] [PubMed]
17. AOAC. *Official Methods of Analysis of the Association of Official's Analytical Chemists*, 14th ed.; Association of Official Analytical Chemist: Washington, DC, USA, 1990; Volume 223–225, pp. 992–995.
18. González Martínez, M.; Anca Couce, A.; Dupont, C.; da Silva Perez, D.; Thiéry, S.; Meyer, X.; Gourdon, C. Torrefaction of Cellulose, Hemicelluloses and Lignin Extracted from Woody and Agricultural Biomass in TGA-GC/MS: Linking Production Profiles of Volatile Species to Biomass Type and Macromolecular Composition. *Ind. Crops Prod.* **2022**, *176*, 114350. [CrossRef]
19. Brebu, M.; Tamminen, T.; Spiridon, I. Thermal Degradation of Various Lignins by TG-MS/FTIR and Py-GC-MS. *J. Anal. Appl. Pyrolysis* **2013**, *104*, 531–539. [CrossRef]
20. Wang, S.; Dai, G.; Yang, H.; Luo, Z. Lignocellulosic Biomass Pyrolysis Mechanism: A State-of-the-Art Review. *Prog. Energy Combust. Sci.* **2017**, *62*, 33–86. [CrossRef]
21. Farrell, R.R.; Wellinger, M.; Gloess, A.N.; Nichols, D.S.; Breadmore, M.C.; Shellie, R.A.; Yeretzyan, C. Real-Time Mass Spectrometry Monitoring of Oak Wood Toasting: Elucidating Aroma Development Relevant to Oak-Aged Wine Quality. *Sci. Rep.* **2015**, *5*, 17334. [CrossRef]
22. Duval, C.J.; Sok, N.; Laroche, J.; Gourrat, K.; Prida, A.; Lequin, S.; Chassagne, D.; Gougeon, R.D. Dry vs Soaked Wood: Modulating the Volatile Extractible Fraction of Oak Wood by Heat Treatments. *Food Chem.* **2013**, *138*, 270–277. [CrossRef]
23. D'Eusanio, V.; Genua, F.; Marchetti, A.; Morelli, L.; Tassi, L. Exploring the Mineral Composition of Grapevine Canes for Wood Chip Applications in Alcoholic Beverage Production to Enhance Viticulture Sustainability. *Beverages* **2023**, *9*, 60. [CrossRef]
24. Official Journal of the European Union Regulation (EC) No 1107/2009 of the European Parliament and of the Council of 21 October 2009 Concerning the Placing of Plant Protection Products on the Market and Repealing Council Directives 79/117/EEC and 91/414/EEC 2009. Official Journal of the European Union. L 309/1. Available online: <https://eur-lex.europa.eu/LexUriServ/LexUriServ.do?uri=OJ:L:2009:309:0001:0050:en:PDF> (accessed on 20 March 2023).
25. Dorosh, O.; Fernandes, V.C.; Moreira, M.M.; Delerue-Matos, C. Occurrence of Pesticides and Environmental Contaminants in Vineyards: Case Study of Portuguese Grapevine Canes. *Sci. Total Environ.* **2021**, *791*, 148395. [CrossRef] [PubMed]
26. Moldes, A.B.; Bustos, G.; Torrado, A.; Domínguez, J.M. Comparison between Different Hydrolysis Processes of Vine-Trimming Waste to Obtain Hemicellulosic Sugars for Further Lactic Acid Conversion. *Appl. Biochem. Biotechnol.* **2007**, *143*, 244–256. [CrossRef] [PubMed]
27. Max, B.; Salgado, J.M.; Cortés, S.; Domínguez, J.M. Extraction of Phenolic Acids by Alkaline Hydrolysis from the Solid Residue Obtained after Prehydrolysis of Trimming Vine Shoots. *J. Agric. Food Chem.* **2010**, *58*, 1909–1917. [CrossRef] [PubMed]
28. Dávila, I.; Gordobil, O.; Labidi, J.; Gullón, P. Assessment of Suitability of Vine Shoots for Hemicellulosic Oligosaccharides Production through Aqueous Processing. *Bioresour. Technol.* **2016**, *211*, 636–644. [CrossRef]
29. Jesus, M.S.; Romani, A.; Genisheva, Z.; Teixeira, J.A.; Domingues, L. Integral Valorization of Vine Pruning Residue by Sequential Autohydrolysis Stages. *J. Clean. Prod.* **2017**, *168*, 74–86. [CrossRef]
30. Blackford, M.; Comby, M.; Zeng, L.; Dienes-Nagy, Á.; Bourdin, G.; Lorenzini, F.; Bach, B. A Review on Stems Composition and Their Impact on Wine Quality. *Molecules* **2021**, *26*, 1240. [CrossRef]
31. McKendry, P. Energy Production from Biomass (Part 1): Overview of Biomass. *Bioresour. Technol.* **2002**, *83*, 37–46. [CrossRef]
32. González-Centeno, M.R.; Rosselló, C.; Simal, S.; Garau, M.C.; López, F.; Femenia, A. Physico-Chemical Properties of Cell Wall Materials Obtained from Ten Grape Varieties and Their Byproducts: Grape Pomaces and Stems. *LWT—Food Sci. Technol.* **2010**, *43*, 1580–1586. [CrossRef]
33. Ping, L.; Brosse, N.; Sannigrahi, P.; Ragauskas, A. Evaluation of Grape Stalks as a Bioresource. *Ind. Crops Prod.* **2011**, *33*, 200–204. [CrossRef]
34. Sánchez-Gómez, R.; Alonso, G.L.; Salinas, M.R.; Zalacain, A. Reuse of Vine-Shoots Wastes for Agricultural Purposes. In *Handbook of Grape Processing By-Products*; Elsevier: Amsterdam, The Netherlands, 2017; pp. 79–104. ISBN 978-0-12-809870-7.
35. Çetin, E.S.; Altinöz, D.; Tarçan, E.; Göktürk Baydar, N. Chemical Composition of Grape Canes. *Ind. Crops Prod.* **2011**, *34*, 994–998. [CrossRef]
36. Mendivil, M.A.; Muñoz, P.; Morales, M.P.; Juárez, M.C.; García-Escudero, E. Chemical Characterization of Pruned Vine Shoots from La Rioja (Spain) for Obtaining Solid Bio-Fuels. *J. Renew. Sustain. Energy* **2013**, *5*, 033113. [CrossRef]
37. Johnson, C.M. Differential Scanning Calorimetry as a Tool for Protein Folding and Stability. *Arch. Biochem. Biophys.* **2013**, *531*, 100–109. [CrossRef] [PubMed]
38. Ojeda-Galván, H.J.; Hernández-Arteaga, A.C.; Rodríguez-Aranda, M.C.; Toro-Vazquez, J.F.; Cruz-González, N.; Ortiz-Chávez, S.; Comas-García, M.; Rodríguez, A.G.; Navarro-Contreras, H.R. Application of Raman Spectroscopy for the Determination of Proteins Denaturation and Amino Acids Decomposition Temperature. *Spectrochim. Acta. A Mol. Biomol. Spectrosc.* **2023**, *285*, 121941. [CrossRef] [PubMed]
39. Şen, D.; Gökmen, V. Kinetic Modeling of Maillard and Caramelization Reactions in Sucrose-Rich and Low Moisture Foods Applied for Roasted Nuts and Seeds. *Food Chem.* **2022**, *395*, 133583. [CrossRef] [PubMed]
40. Weiss, I.M.; Muth, C.; Drumm, R.; Kirchner, H.O.K. Thermal Decomposition of the Amino Acids Glycine, Cysteine, Aspartic Acid, Asparagine, Glutamic Acid, Glutamine, Arginine and Histidine. *BMC Biophys.* **2018**, *11*, 2. [CrossRef] [PubMed]
41. Salema, A.A.; Ting, R.M.W.; Shang, Y.K. Pyrolysis of Blend (Oil Palm Biomass and Sawdust) Biomass Using TG-MS. *Bioresour. Technol.* **2019**, *274*, 439–446. [CrossRef]

42. Ding, Y.; Huang, B.; Li, K.; Du, W.; Lu, K.; Zhang, Y. Thermal Interaction Analysis of Isolated Hemicellulose and Cellulose by Kinetic Parameters during Biomass Pyrolysis. *Energy* **2020**, *195*, 117010. [CrossRef]
43. Yang, H.; Yan, R.; Chin, T.; Liang, D.T.; Chen, H.; Zheng, C. Thermogravimetric Analysis—Fourier Transform Infrared Analysis of Palm Oil Waste Pyrolysis. *Energy Fuels* **2004**, *18*, 1814–1821. [CrossRef]
44. Zhao, C.; Jiang, E.; Chen, A. Volatile Production from Pyrolysis of Cellulose, Hemicellulose and Lignin. *J. Energy Inst.* **2017**, *90*, 902–913. [CrossRef]
45. Yeo, J.Y.; Chin, B.L.F.; Tan, J.K.; Loh, Y.S. Comparative Studies on the Pyrolysis of Cellulose, Hemicellulose, and Lignin Based on Combined Kinetics. *J. Energy Inst.* **2019**, *92*, 27–37. [CrossRef]
46. Wei, M.; Ma, T.; Ge, Q.; Li, C.; Zhang, K.; Fang, Y.; Sun, X. Challenges and Opportunities of Winter Vine Pruning for Global Grape and Wine Industries. *J. Clean. Prod.* **2022**, *380*, 135086. [CrossRef]
47. Hofmann, T.; Schieberle, P. Formation of Aroma-Active Strecker-Aldehydes by a Direct Oxidative Degradation of Amadori Compounds. *J. Agric. Food Chem.* **2000**, *48*, 4301–4305. [CrossRef] [PubMed]
48. Gernat, D.C.; Brouwer, E.; Ottens, M. Aldehydes as Wort Off-Flavours in Alcohol-Free Beers—Origin and Control. *Food Bioprocess Technol.* **2020**, *13*, 195–216. [CrossRef]
49. Gehlken, J.; Pour Nikfardjam, M.; Zörb, C. Prediction of Sensory Attributes in Winemaking Grapes by On-Line near-Infrared Spectroscopy Based on Selected Volatile Aroma Compounds. *Anal. Bioanal. Chem.* **2023**, *415*, 1515–1527. [CrossRef] [PubMed]
50. Berger, R.G. *Flavours and Fragrances: Chemistry, Bioprocessing and Sustainability*; Springer: Berlin/Heidelberg, Germany, 2007; ISBN 978-3-540-49338-9.
51. Liu, J.; Wan, P.; Xie, C.; Chen, D.-W. Key Aroma-Active Compounds in Brown Sugar and Their Influence on Sweetness. *Food Chem.* **2021**, *345*, 128826. [CrossRef] [PubMed]
52. Lin, X.; Sui, S.; Tan, S.; Pittman, C.U.; Sun, J.; Zhang, Z. Fast Pyrolysis of Four Lignins from Different Isolation Processes Using Py-GC/MS. *Energies* **2015**, *8*, 5107–5121. [CrossRef]
53. Shen, D.; Liu, G.; Zhao, J.; Xue, J.; Guan, S.; Xiao, R. Thermo-Chemical Conversion of Lignin to Aromatic Compounds: Effect of Lignin Source and Reaction Temperature. *J. Anal. Appl. Pyrolysis* **2015**, *112*, 56–65. [CrossRef]
54. Tipparaju, S.; Ravishankar, S.; Slade, P.J. Survival of *Listeria Monocytogenes* in Vanilla-Flavored Soy and Dairy Products Stored at 8 °C. *J. Food Prot.* **2004**, *67*, 378–382. [CrossRef]
55. Ngarmsak, M.; Delaquis, P.; Toivonen, P.; Ngarmsak, T.; Oraikul, B.; Mazza, G. Antimicrobial Activity of Vanillin against Spoilage Microorganisms in Stored Fresh-Cut Mangoes. *J. Food Prot.* **2006**, *69*, 1724–1727. [CrossRef]
56. Durant, S. Vanillins—A Novel Family of DNA-PK Inhibitors. *Nucleic Acids Res.* **2003**, *31*, 5501–5512. [CrossRef]
57. Bezerra, D.P.; Soares, A.K.N.; De Sousa, D.P. Overview of the Role of Vanillin on Redox Status and Cancer Development. *Oxid. Med. Cell. Longev.* **2016**, *2016*, 9734816. [CrossRef] [PubMed]
58. Bosman, R.N.; Lashbrooke, J.G. Grapevine Mono- and Sesquiterpenes: Genetics, Metabolism, and Ecophysiology. *Front. Plant Sci.* **2023**, *14*, 1111392. [CrossRef] [PubMed]
59. Bartikova, H.; Hanusova, V.; Skalova, L.; Ambroz, M.; Bousova, I. Antioxidant, Pro-Oxidant and Other Biological Activities of Sesquiterpenes. *Curr. Top. Med. Chem.* **2014**, *14*, 2478–2494. [CrossRef] [PubMed]
60. Wu, Y.; Duan, S.; Zhao, L.; Gao, Z.; Luo, M.; Song, S.; Xu, W.; Zhang, C.; Ma, C.; Wang, S. Aroma Characterization Based on Aromatic Series Analysis in Table Grapes. *Sci. Rep.* **2016**, *6*, 31116. [CrossRef] [PubMed]
61. Parker, M.; Pollnitz, A.P.; Cozzolino, D.; Francis, I.L.; Herderich, M.J. Identification and Quantification of a Marker Compound for ‘Pepper’ Aroma and Flavor in Shiraz Grape Berries by Combination of Chemometrics and Gas Chromatography—Mass Spectrometry. *J. Agric. Food Chem.* **2007**, *55*, 5948–5955. [CrossRef] [PubMed]
62. Ulrich, D.; Hoberg, E.; Bittner, T.; Engewald, W.; Meilchen, K. Contribution of Volatile Compounds to the Flavor of Cooked Asparagus. *Eur. Food Res. Technol.* **2001**, *213*, 200–204. [CrossRef]
63. Duckham, S.C.; Dodson, A.T.; Bakker, J.; Ames, J.M. Volatile Flavour Components of Baked Potato Flesh. A Comparison of Eleven Potato Cultivars. *Nahr.* **2001**, *45*, 317–323. [CrossRef]
64. Cerny, C. 9—The Role of Sulfur Chemistry in Thermal Generation of Aroma. In *Flavour Development, Analysis and Perception in Food and Beverages*; Parker, J.K., Elmore, J.S., Methven, L., Eds.; Woodhead Publishing Series in Food Science, Technology and Nutrition; Woodhead Publishing: Sawston, UK, 2015; pp. 187–210. ISBN 978-1-78242-103-0.
65. Naeher, L.P.; Brauer, M.; Lipsett, M.; Zelikoff, J.T.; Simpson, C.D.; Koenig, J.Q.; Smith, K.R. Woodsmoke Health Effects: A Review. *Inhal. Toxicol.* **2007**, *19*, 67–106. [CrossRef]
66. IARC—International Agency for Research on Cancer. Available online: <https://www.iarc.who.int/> (accessed on 12 April 2023).
67. Bird, M.G.; Greim, H.; Snyder, R.; Rice, J.M. International Symposium: Recent Advances in Benzene Toxicity. *Chem. Biol. Interact.* **2005**, *153–154*, 1–5. [CrossRef]
68. Salviano dos Santos, V.P.; Medeiros Salgado, A.; Guedes Torres, A.; Signori Pereira, K. Benzene as a Chemical Hazard in Processed Foods. *Int. J. Food Sci.* **2015**, *2015*, 545640. [CrossRef]

**Disclaimer/Publisher’s Note:** The statements, opinions and data contained in all publications are solely those of the individual author(s) and contributor(s) and not of MDPI and/or the editor(s). MDPI and/or the editor(s) disclaim responsibility for any injury to people or property resulting from any ideas, methods, instructions or products referred to in the content.